J Mater Sci: Mater Electron (2009) 20:253–256
DOI 10.1007/s10854-008-9712-3

Electrical and optical properties of ZnO:Al thin films grown by magnetron sputtering

Shr-Nan Bai · Tseung-Yuen Tseng

Received: 1 December 2007 / Accepted: 20 March 2008 / Published online: 17 April 2008

Abstract The properties of transparent conductive ZnO:Al thin films grown by R.F. magnetron sputtering method are investigated. The working pressure (argon gas) is changed from 2.5 to 40.0 mTorr to study its influence on the characteristics of ZnO:Al thin films. The ZnO:Al thin films have better texture due to the increase in the surface mobility, which resulted from the increase in the mean free path of sputtering gas under lower working pressure. The microstructure of ZnO:Al films is found to be affected obviously by changing the working pressure. It is shown that the grain size of ZnO:Al thin films decreases with the increase of working pressure. The X-ray diffraction patterns indicate that the poor crystallized structure of ZnO:Al films is obtained at higher working pressure. Except 40 mTorr, the highly (002)-oriented ZnO:Al thin films can be found at the measured range of working pressure. Moreover, the growth rate of the films decreases from 1.5 to 0.5 nm/min as the working pressure increases from 2.5 to 40.0 mTorr. The results of optical transmittance measurement of ZnO:Al thin films reveal a high transmittance (>80%) in visible region and exhibit a sharp absorption edge at wavelength about 350 nm.

S.-N. Bai (✉)
Department of Electronic Engineering, Institute of Electronic, Chienkuo Technology University, Changhua City 500, Taiwan, ROC
e-mail: snbai@ctu.edu.tw

T.-Y. Tseng
Department of Electronics Engineering, Institute of Electronics, National Chiao-Tung University, Hsinchu City 300, Taiwan, ROC
e-mail: tseng@cc.nctu.edu.tw

1 Introduction

The inexpensive and nontoxic zinc oxide (ZnO) based materials have attracted a lot of attentions as the transparent conductive material in recent years due to the extreme commercial interest in progressing flat panel display, solar cell, and other different optoelectronic devices [1–5]. The ZnO-based materials are also promising for application as an ultraviolet and blue light emitter because of sufficiently large excitation binding energy of 60 meV, which is stable even at room temperature. There were many techniques employed to grow ZnO-based thin films, including magnetron sputtering [6, 7], pulsed laser deposition [8], reactive electron-beam evaporation [9, 10], metalorganic chemical vapor deposition [11], metallic zinc oxidation [12], spray pyrolysis [13–15], and molecular beam epitaxy [16]. For all of these deposition techniques, sputtering technology is the most commonly used method because it can obtain good orientation and uniform thickness films at low substrate temperature or even on amorphous substrate. Krikorian et al. [17] have mentioned that three critical factors determining epitaxial growth in sputtering for a given material are background pressure, substrate temperature, and deposition rate. Under the various growth conditions such as substrate temperature, annealing temperature, and various substrates, the growth of ZnO-based thin films has been widely investigated [18–21]. However, the influence of working pressure on the electrical and optical characteristics of ZnO-based thin films is rarely found in the published literatures. In this investigation, a careful planning study of the effect of working pressure on the properties of R.F. magnetron sputtered ZnO:Al thin films is presented. The relationship between film characteristics and working pressure is also reported.

2 Experimental

The transparent conductive Al_2O_3-doped ZnO (ZnO:Al) films were grown on 1737F Corning glass substrate by R.F. magnetron sputtering system operating at room temperature with a power of 50 W. The substrate was ultrasonically cleaned in acetone, alcohol, and D.I. water. A three-inch circular shape target of ZnO (purity, 99.99%) mixed with 2 wt.% Al_2O_3 (purity, 99.99%) was employed. The sputtering chamber was evacuated to 8×10^{-6} Torr through a mass flow controller. Then, the high purity Ar gas with pressure ranges varied from 2.5 to 40.0 mTorr was used to evaluate the influence of the working pressure on structural, electrical, and optical characteristics of the ZnO:Al thin films. Prior to the ZnO:Al films deposition, the pre-sputtering for 10 min was carried out in order to clean the target's surface contamination.

The surface morphology and microstructure of the ZnO:Al films were studied using the high-resolution cold field emission scanning electron microscope (FE-SEM). The crystalline structure and orientation of the ZnO:Al thin films were analyzed by X-ray diffraction (XRD). The film thickness was determined from SEM images of the fracture cross-section area of the ZnO:Al films. The electrical resistivities were determined by the van der Pauw method. An electric current was applied through electrodes and each potential difference between the electrodes was measured. The electric resistivities were calculated from I–V curves by the least-squares method. The optical transmission spectra through the ZnO:Al thin films were recorded using an ultraviolet-visible spectrophotometer in the wavelength range of 200–800 nm.

3 Results and discussion

Figure 1a and b shows the SEM micrographs of ZnO:Al thin films prepared at working pressure of 2.5 and 20.0 mTorr. It can be seen that the grain size of the films deposited at various working pressures is quite different. In Fig. 1a and b, the grain size is decreased with an increase of working pressure. The higher working pressure may result in lower growth rate, smaller grain sizes and worse crystallinity. An increasing in working pressure can increase the sputtering rate and at the same time lower the energy of sputtered particles, and therefore as a result of the competing effects. The working pressure demonstrates a noticeable effect on the microstructure of ZnO:Al thin films in this study. The sputtered materials possess a mean free path that is comparable to the distance in which from target to substrate at lower pressure. These arriving materials, at lower pressure, have much higher energy that results in higher surface mobility and thus a much larger possibility to form ZnO:Al thin films.

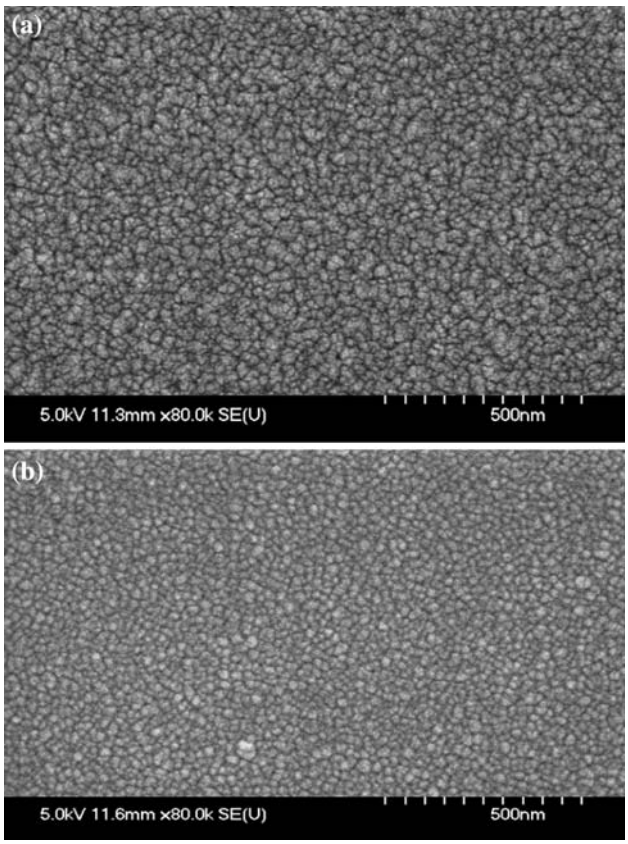

Fig. 1 SEM images of ZnO:Al thin films deposited at (**a**) 2.5 mTorr, (**b**) 20.0 mTorr

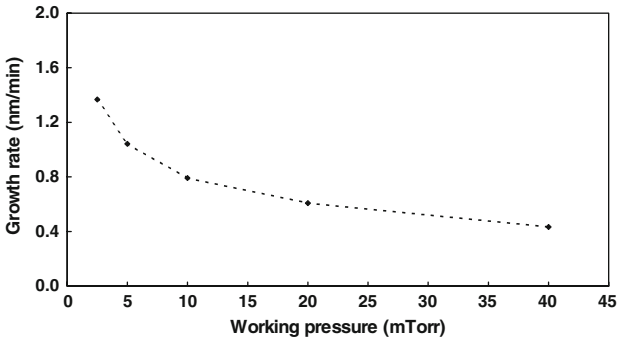

Fig. 2 Growth rate of ZnO:Al thin films as a function of working pressure

Figure 2 demonstrates the growth rate of ZnO:Al films prepared with different working pressures. The average growth rate was calculated based on the mean value of thickness from the cross-section images of the thin films. It is found that the growth rate of the ZnO:Al films is quite sensitive to the working pressure of vacuum chamber. The growth rate is decreased with increasing of working pressure in the range from 2.5 to 40.0 mTorr. The decrease of growth rate with an increase of working pressure can be

explained that the sputtered materials have no sufficiently energy due to the mean free path of the materials is smaller than the distance from target to substrate at higher pressure [22]. In addition, the collision probabilities of the depositing materials increase under higher working pressure; therefore, the sputtering rate decreases and results in the growth rate of ZnO:Al thin films decreases as the working pressure increases.

Figure 3 demonstrates the XRD patterns of ZnO:Al thin films deposited at working pressure of 2.5–40.0 mTorr. It is found that the intensity of the peaks is decreased with increasing of working pressure. All of the sputtered films exhibit preferential (002) orientation with c-axis perpendicular to the substrate surface, except the film prepared at 40 mTorr. Based on previous SEM and growth rate experimental results, the higher the working pressure, the thinner the ZnO films become. When the ZnO films are very thin, the lattice mismatches and crystal growth competition among the adjacent crystal islands will exist and these imperfections cause the intensity of (002) diffraction peak becomes weakened or even disappeared. The peak disappears at 40 mTorr of working pressure actually indicating that the microstructure of the film is amorphous. The ZnO:Al thin films deposited on glass substrate show only the (002) peak in the measured 2θ region and no diffraction peaks from randomly oriented grains or other impurity phases are presented. Supposing a uniform strain across the deposited film, the size of the crystallites D in the grains can be estimated by the Scherrer's formula [23]:

$$D = \frac{k\lambda}{B\cos\theta}$$

where k is the shape factor of the crystallite (expected shape factor is 0.9), λ the X-ray wavelength, B the full width at half maximum (FWHM) of the (002) diffraction peak, and θ the Bragg diffraction angle. The estimated values of the ZnO average grain size with working pressures of 2.5, 5, 10, and 20 mTorr are 19.8, 19.3, 15.4, and 12.2 nm, respectively.

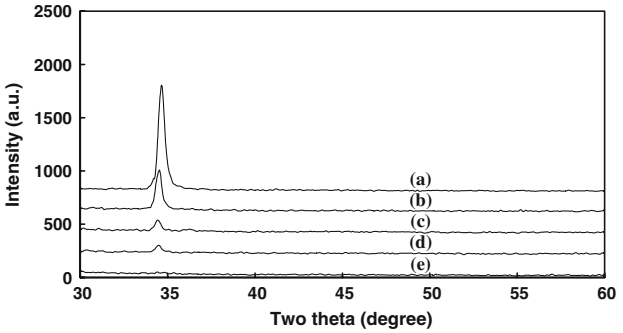

Fig. 3 X-ray diffraction spectra of ZnO:Al thin films deposited at various working pressures (**a**) 2.5 mTorr, (**b**) 5 mTorr, (**c**) 10 mTorr, (**d**) 20 mTorr, (**e**) 40 mTorr

Figure 4 shows the influence of working pressure on the electrical resistivity of the ZnO:Al thin films. It can be observed that the resistivity increases with an increase of working pressure. The resistivity is increased from 4.1×10^{-3} to 5.2×10^{-1} ohm·cm as the working pressure is increased from 2.5 to 40.0 mTorr. The electrical resistivity is well known proportional to the reciprocal of the product of the carrier concentration and the mobility. Therefore, the variation in resistivity with working pressure maybe attributed to the change in carrier concentration and/or mobility. ZnO is typically an *n*-type semiconductor in which has high conductivity mainly from stoichiometric deviation. The electrical conductivity of ZnO:Al films is higher than that of pure ZnO films because that the contribution from Al^{3+} ions on substitutional sites of Zn^{2+} ions acts as donor. Therefore, it can be reasonably suggested that the ZnO:Al films deposited under higher working pressure may have less carrier concentration causing the electrical conductivity of the ZnO:Al thin films lower. Besides, the ZnO:Al films are extremely chemically active. The chemisorption of oxygen atoms at the surface of ZnO:Al thin films may absorb electrons from the conduction band and therefore reduces the carrier concentration and then broadens the depletion layers within the ZnO grain boundaries [24]. Additionally, it has been shown earlier that the growth rate is decreased with increasing of working pressure. The average grain size of the ZnO:Al films is smaller at a higher working pressure, which increases the grain-boundary scattering and thus decreases the mobility. Therefore, it can be summarized that the increase of electrical resistivity of ZnO:Al thin films with increasing working pressure is due to the decrease in the carrier concentration and mobility.

Figure 5 demonstrates the optical transmission spectra of ZnO:Al films as a function of wavelength prepared at various working pressures. The average optical transmittance in the visible region is above 80% for all of the films and decreases with an increase in working pressure. According to the cross-section images of the ZnO:Al thin

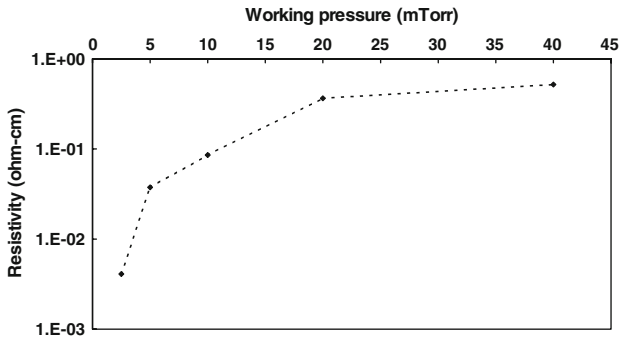

Fig. 4 Electrical resistivity of ZnO:Al thin films as a function of working pressure

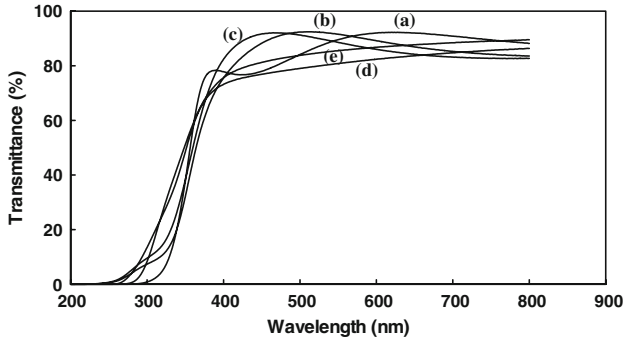

Fig. 5 Optical transmittance spectra of ZnO:Al thin films deposited at various working pressures (**a**) 2.5 mTorr, (**b**) 5 mTorr, (**c**) 10 mTorr, (**d**) 20 mTorr, (**e**) 40 mTorr

films, the thickness of the films decreases as the working pressure is increased. The thickness of the ZnO:Al thin films with working pressure of 2.5, 5, 10, 20 and 40 mTorr is 164, 125, 95, 73, and 52 nm, respectively. At higher working pressures, the composition of the ZnO:Al becomes much nonstoichiometric and their grain sizes decrease. It results in the light scattering loss and the destruction of coherence between incident light and reflected light and therefore leads to the disappearance of interference fringes as well as the decrease in transmittance.

4 Conclusions

It is found that the structural, electrical, and optical properties of the sputtered ZnO:Al thin films depend on working pressure. The SEM observation shows that the grain size is decreased with an increase of working pressure. It implied that the growth rate decreases with increasing working pressure. This is attributed to the decrease in the surface mobility, which caused by the decrease in the mean free path of sputtering gas, under higher working pressure. The XRD results show that the ZnO:Al thin films deposited on glass substrate at different working pressures demonstrate only the (002) peak in the displayed 2θ region. The study on the electrical resistivity of ZnO:Al films prepared at higher working pressures reveal that the films with smaller grain size have more grain-boundary scattering that lowers the electrical conductivity of the ZnO:Al films. Moreover, the chemisorption of oxygen atoms at the surface of ZnO:Al thin films is an another possible factor to affect the resistivity. The optical transmission studies demonstrate that the average optical transmittance in the visible region is above 80% for all of the films and decreases with an increase in working pressure.

Acknowledgements The authors appreciate the financial support from the National Science Council, Taiwan, Republic of China, under Project Numbers NSC 95-2221-E-009-120 and NSC 95-2221-E-270-018. Mr. F. C. Chuang is thanked for his help in experimental works.

References

1. B.Y. Oh, M.C. Geong, T.H. Moon, W. Lee, J.M. Myoung, J.Y. Hwang, D.S. Seo, J. Appl. Phys. **99**, 124505–124508 (2006)
2. Y.W. Zhu, H.Z. Zhang, X.C. Sun, S.Q. Feng, J. Xu, Q. Zhao, B. Xiang, R.M. Wang, D.P. Yu, Appl. Phys. Lett. **83**, 144–146 (2003). doi:10.1063/1.1589166
3. E. Hosono, S. Fujihara, I. Honma, H. Zhou, Adv. Mater. **17**, 2091–2094 (2005). doi:10.1002/adma.200500275
4. B. Sang, A. Yamada, M. Konagai, Jpn. J. Appl. Phys. **37**, L206–L208 (1998). doi:10.1143/JJAP.37.L206
5. D. Wang, C. Song, J. Phys. Chem. B **109**, 12697–12700 (2005). doi:10.1021/jp0506134
6. A.N. Banerjee, C.K. Ghosh, K.K. Chattopadhyay, H. Minoura, A.K. Sarkar, A. Akiba, A. Kamiya, T. Endo, Thin Solid Films **496**, 112–116 (2006). doi:10.1016/j.tsf.2005.08.258
7. X. Yu, J. Ma, F. Ji, Y. Wang, X. Zhang, C. Cheng, H. Ma, J. Cryst. Growth **274**, 474–479 (2005). doi:10.1016/j.jcrysgro.2004.10.037
8. J. PerrieÌre, E. Millon, W. Seiler, C. Boulmer-Leborgne, V. Craciun, O. Albert, J.C. Loulergue, J. Etchepare, J. Appl. Phys. **91**, 690–696 (2002). doi:10.1063/1.1426250
9. R. Al Asmar, G. Ferblantier, F. Mailly, P. Gall-Borrut, A. Foucaran, Thin Solid Films **473**, 49–53 (2005). doi:10.1016/j.tsf.2004.06.156
10. H.Z. Wu, K.M. He, D.J. Qiu, D.M. Huang, J. Cryst. Growth **217**, 131–137 (2000). doi:10.1016/S0022-0248(00)00397-3
11. B.P. Zhang, K. Wakatsuki, N.T. Binh, N. Usami, Y. Segawa, Thin Solid Films **449**, 12–19 (2004). doi:10.1016/S0040-6090(03)01466-4
12. A. Umar, S.H. Kim, Y.H. Im, Y.B. Hahn, Superlattices Microstruc. **39**, 238–246 (2006). doi:10.1016/j.spmi.2005.08.046
13. S.A. Studenikin, N. Golego, M. Cocivera, J. Appl. Phys. **83**, 2104–2111 (1998). doi:10.1063/1.366944
14. A. Bougrine, A. El Hichou, M. Addou, J. Ebotheì, A. Kachouane, M. Troyon, Mater. Chem. Phys. **80**, 438–445 (2003). doi:10.1016/S0254-0584(02)00505-9
15. M. Miki-Yoshida, F. Paraguay-Delgado, W. Estrada-Loìpez, E. Andrade, Thin Solid Films **376**, 99–109 (2000). doi:10.1016/S0040-6090(00)01408-5
16. Z. Jin, T. Fukumura, M. Kawasaki, K. Ando, H. Saito, T. Sekiguchi, Y.Z. Yoo, M. Murakami, Y. Matsumoto, T. Hasegawa, H. Koinuma, Appl. Phys. Lett. **78**, 3824–3826 (2001). doi:10.1063/1.1377856
17. E. Krikorian, R.J. Sneed, Astrophys. Space Sci. **65**, 129–154 (1979). doi:10.1007/BF00643495
18. E.G. Fu, D.M. Zhuang, G. Zhang, W.F. Yang, M. Zhao, Appl. Surf. Sci. **217**, 88–94 (2003). doi:10.1016/S0169-4332(03)00523-3
19. V. Gupta, A. Mansingh, J. Appl. Phys. **80**, 1063–1073 (1996). doi:10.1063/1.362842
20. C.H. Choi, S.H. Kim, J. Cryst. Growth **283**, 170–179 (2005). doi:10.1016/j.jcrysgro.2005.05.050
21. V. Srikant, D.R. Clarke, J. Appl. Phys. **81**, 6357–6364 (1997). doi:10.1063/1.364393
22. N. Saito, Y. Igasaki, Appl. Surf. Sci. **169/170**, 349–352 (2001). doi:10.1016/S0169-4332(00)00676-0
23. H.P. Klug, L.E. Alexander, X-Ray Diffraction Procedures for Polycrystalline and Amorphous Materials, 2nd edn. (Wiley-Interscience, New York, 1974), pp. 687–690
24. S.N. Bai, T.Y. Tseng, J. Am. Ceram. Soc. **78**, 2685–2689 (1995). doi:10.1111/j.1151-2916.1995.tb08041.x